Supporting Information

Optical Property, Oxidative Potential and Chemical Composition of Brown Carbon in the Megacity Shenyang of Northeast China

Jianwei Zheng[a], Wangjin Yang[a,*], Hao Na[a], Hongxing Yang[a], Fu Li[a], Shaojie Yang[a], Ning Tang[b], Chong Han[a,*]

[a] School of Metallurgy, Northeastern University, Shenyang, 110819, China

[b] Institute of Nature and Environmental Technology, Kanazawa University, Kanazawa 920-1192, Japan

*To Whom Correspondence Should Be Addressed:

hanch@smm.neu.edu.cn; yangwj@smm.neu.edu.cn

Summary

29 Table S1. The structural formula of target compounds.

Type	Compounds	Structural formula
Polycyclic aromatic hydrocarbons (PAHs)	Phenanthrene (Phe)	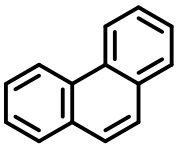
	Fluorene (Flu)	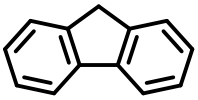
	Fluoranthene (Fla)	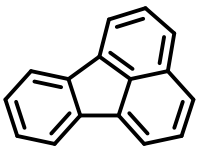
	Pyrene (Pyr)	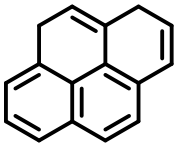
	Perylene (Per)	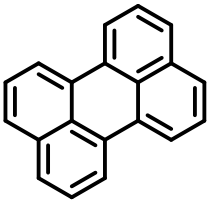
Oxygenated polycyclic aromatic hydrocarbons (OPAHs)	Anthraquinone (AQ)	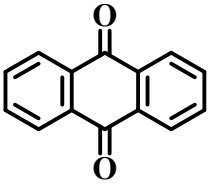
	Naphthalene-1,4-Dione (1,4-NQ)	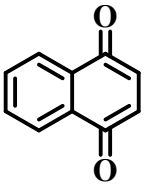
	9-Fluorenone (9-Flu)	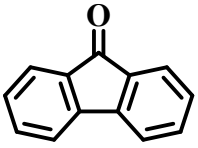
	1,4-Anthraquinone (1,4-AQ)	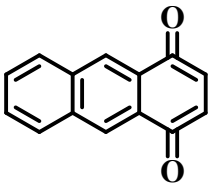

OPAHs	9,10-Phenanthraquinone (9,10-PQ)	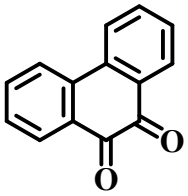
Nitrated polycyclic aromatic hydrocarbons (NPAHs)	5-Nitracenaphthene (5-NAce)	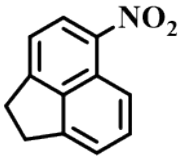
	2-Nitrofluorene (2-NF)	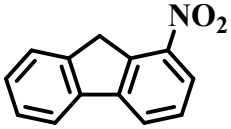
	2,7-Dinitrofluorene (2,7-DNF)	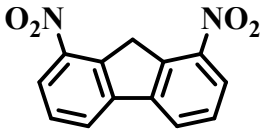
	9-Nitroanthracene (9-NAnt)	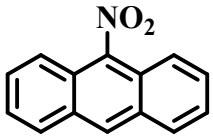
	1-Nitropyrene (1-NP)	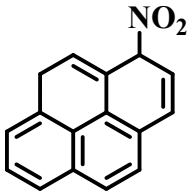

Table S2. Sampling dates of $PM_{2.5}$.

Seasons	Sampling dates
Spring (Spr)	25–27 May. 2023
Summer (Sum)	21–23 Aug. 2023
Autumn (Aut)	9–11 Nov. 2023
Winter (Win)	9–11 Feb. 2023

Table S3. Meteorological conditions of the sampling days.

Date	Temperature (°C)	Mean relative humidity (%)	Mean wind speed (m s^{-1})
25 May. 2023	16.30 ~ 22.30	47.20	4.90
26 May. 2023	12.80 ~ 27.10	65.00	2.50
27 May. 2023	12.10 ~ 23.70	69.90	2.40
21 Aug. 2023	21.50 ~ 25.10	84.10	1.50
22 Aug. 2023	15.60 ~ 28.00	80.80	1.00
23 Aug. 2023	17.20 ~ 29.40	75.20	1.10
9 Nov. 2023	–5.60 ~ 0.20	52.30	3.10
10 Nov. 2023	–11.10 ~ –3.00	65.20	1.40
11 Nov. 2023	–12.20 ~ –2.50	66.40	1.40
9 Feb. 2023	–9.30 ~ 2.80	47.90	1.40
10 Feb. 2023	–8.10 ~ 2.90	81.70	1.40
11 Feb. 2023	–5.30~3.80	68.90	2.10

Table S4. The concentration of inorganic salts and metal ions in WSBrC.

Type	Ions	Concentration (mg L^{-1})
Inorganic salts ions	F^-	3.61
	Cl^-	71.60
	NO_2^-	0.99
	Br^-	2.75
	SO_4^{2-}	89.00
	NO_3^-	122.00
	$C_2O_4^{2-}$	1.07
	PO_4^{2-}	0.34
Metal ions	Fe^{2+}	0.47
	Fe^{3+}	0.25
	Mn^{2+}	1.17

Text S1. GC-MS analysis of target compounds

The concentrations of PAHs and their derivatives were quantified using the external calibration method. Standards with the concentrations of 0.25, 0.50, 0.75 and 1.00 μg mL^{-1} were prepared, and multi-point calibration curves were constructed (Area = slope × C_{TC} + intercept). C_{TC} represents the concentrations of target compounds. The linear regressions all showed excellent correlation (R^2 = 0.994–0.999; Table S4), confirming the reliability of quantification. The concentration of target compounds in the BrC extract were calculated from the calibration equation and then converted to ambient concentration using sampling volumes.

Spike recovery experiments were conducted using blank quartz fiber filters as the matrix. A known amount of standard solution containing target compounds was added dropwise onto pre-baked blank filters, and the solvent was evaporated under a gentle stream of N_2. The spiked filters were then extracted, filtered and analyzed using the same procedure as real samples. Recoveries were calculated as the ratio of the measured concentration to the spiked concentration, with average values ranging from 89% to 101% for the target compounds (Table S5).

$$Recovery = \frac{C_{\text{measured}}}{C_{\text{spiked}}} 100\% \quad \text{(S1)}$$

The measurement uncertainty was assessed following established analytical guidance. Major sources of uncertainty included errors associated with calibration regression parameters, instrumental repeatability, recovery variability, extraction and sampling volumes, and dilution factors. These contributions were combined by error propagation to derive a combined standard uncertainty, which expanded with a coverage factor of k = 2, yielded an overall uncertainty of approximately ±10%. This level of uncertainty was within the acceptable range for the quantitative analysis of trace organic pollutants in atmospheric samples.

Table S5. Standard curves of peak area (A) as a function of concentration (μg mL^{-1}), characteristic ions and recoveries (R, %) for the target compounds.

Compounds	Standard curves	m/z	R (%)
Phe	$A = 1615884.91\ C_{TC} - 6155.36$, $R^2 = 0.997$	178	95
Flu	$A = 943744.25\ C_{TC} - 1203.11$, $R^2 = 0.999$	166	96
Fla	$A = 1497641.60\ C_{TC} - 3939.00$, $R^2 = 0.998$	202	100
Pyr	$A = 1518207.60\ C_{TC} + 35776.00$, $R^2 = 0.996$	202	101
Per	$A = 1733254.00\ C_{TC} - 41725.00$, $R^2 = 0.998$	252	99
1,4-NQ	$A = 474697.60\ C_{TC} - 8498.50$, $R^2 = 0.996$	158	90
1,4-AQ	$A = 254565.60\ C_{TC} - 1754.50$, $R^2 = 0.999$	216	92
AQ	$A = 854414.80\ C_{TC} + 9878.00$, $R^2 = 0.994$	180	89
9,10-PQ	$A = 350875.20\ C_{TC} - 759.00$, $R^2 = 0.998$	208	94
9-Flu	$A = 1080108.40\ C_{TC} - 16847.50$, $R^2 = 0.998$	180	91
1-NP	$A = 271550.00\ C_{TC} + 1787.00$, $R^2 = 0.998$	201	99
2-NF	$A = 327755.60\ C_{TC} + 5415.50$, $R^2 = 0.999$	165	97
2,7-DNF	$A = 309962.40\ C_{TC} + 1697.00$, $R^2 = 0.998$	164	99
5-NAce	$A = 284143.60\ C_{TC} + 5567.00$, $R^2 = 0.998$	152	100
9-NAnt	$A = 375437.60\ C_{TC} + 4257.00$, $R^2 = 0.999$	223	101

Table S6. The assignment of FT-IR peaks of BrC.

Wavenumber (cm^{-1})	Functional groups
> 3000	Stretching of O−H in carboxyl, phenol and alcohol
2934, 2930, 2925, 2924, 2920	Asymmetric stretching of C−H
2857, 2854, 2852, 2850	Symmetric stretching of C−H
1735, 1730, 1728, 1717, 1688	Stretching of C=O in carboxylic acid
1645, 1620, 1615, 1606, 1600	Stretching of C=O in quinone and ketone
1531, 1460, 1442, 1436, 1420, 1404, 1400	Stretching of methyl C−H
1384, 1335, 1332, 1280	Stretching of C−NO_2
1240, 1200, 1171	Stretching of aromatic C−O in phenol
1150, 1131, 1120, 1067	Stretching of C−O in polysaccharides
867, 825, 824, 814, 808, 805	Out-of-plane bending of aromatic C−H

Table S7. The C−H peak area (cm^{-1}) and C−H peak area per unit mass of organic carbon (C−H_m, cm^{-1} μg^{-1}) of BrC.

Type	C−H area (cm^{-1})	C−H_m (cm^{-1} μg^{-1})
MSBrC	16.1	0.07
MIBrC	2.07	0.05
WISBrC	40.7	0.89
WSBrC	5.25	0.03
HULIS-n	3.70	0.03
HULIS-a	2.97	0.06
HPWSBrC	2.96	0.18

Table S8. The molecular formula, concentration (ng m^{-3}) and MAE_{365} (m^2 g^{-1}) of target compounds.

Target compounds	Molecular formula	Concentration (ng m^{-3})	MAE_{365} (m^2 g^{-1})
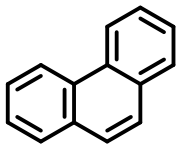 Phe	$C_{14}H_{10}$	6.47	/
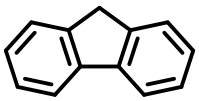 Flu	$C_{13}H_{10}$	3.46	0.02
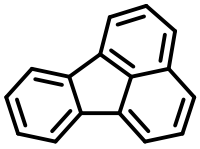 Fla	$C_{16}H_{10}$	18.9	5.54
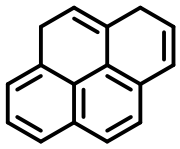 Pyr	$C_{16}H_{10}$	18.10	/
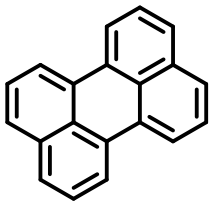 Per	$C_{20}H_{12}$	5.61	2.24
ΣPAHs	/	52.50	/
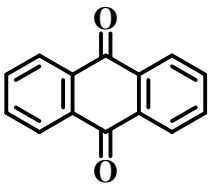 AQ	$C_{14}H_8O_2$	1.00	0.33

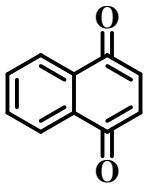 1,4-NQ	$C_{10}H_6O_2$	0.69	0.92
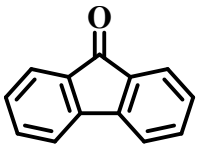 9-Flu	$C_{13}H_8O$	12.20	0.28
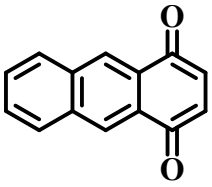 1,4-AQ	$C_{14}H_8O_2$	0.79	1.76
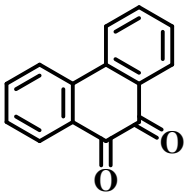 9,10-PQ	$C_{14}H_8O_2$	3.00	1.81
ΣOPAHs	/	17.70	/
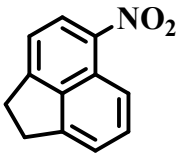 5-NAce	$C_{12}H_9NO_2$	8.00	8.25
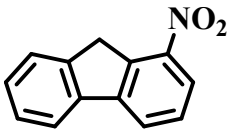 2-NF	$C_{13}H_9NO_2$	5.00	9.56
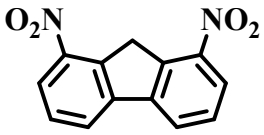 2,7-DNF	$C_{13}H_8N_2O_4$	1.16	13.20

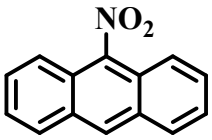 9-NAnt	$C_{14}H_9NO_2$	0.86	5.24
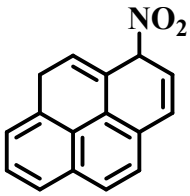 1-NP	$C_{16}H_9NO_2$	8.24	11.10
ΣNPAHs	/	23.30	/
ΣTotal	/	93.50	/

73

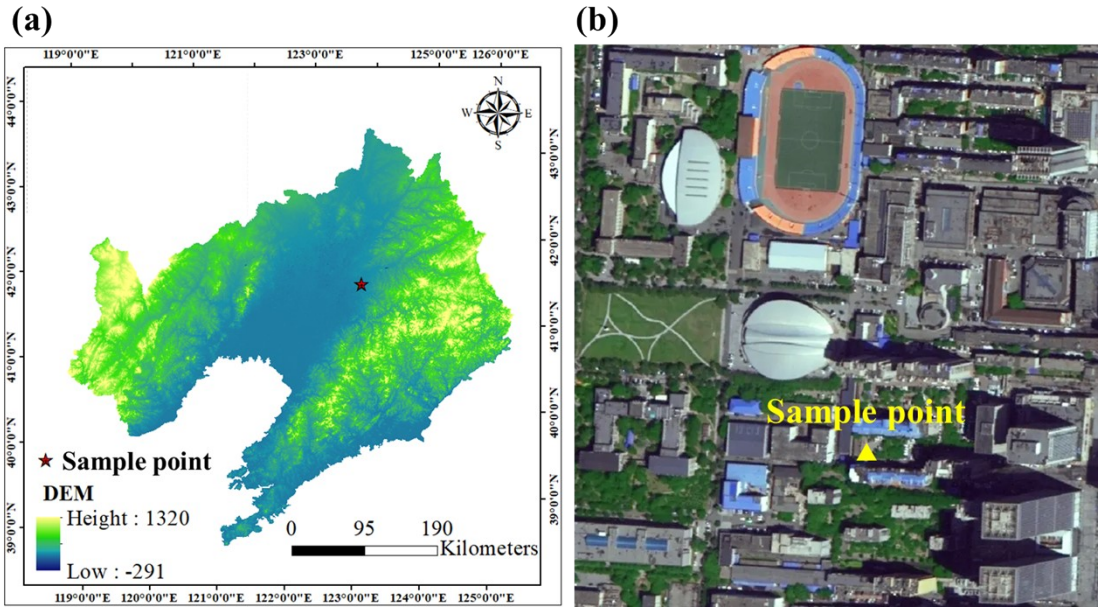

Fig. S1. Geographical coordinates and digital elevation model (DEM) of the sampling point in Liaoning province (a). Overhead view of sample point (b).

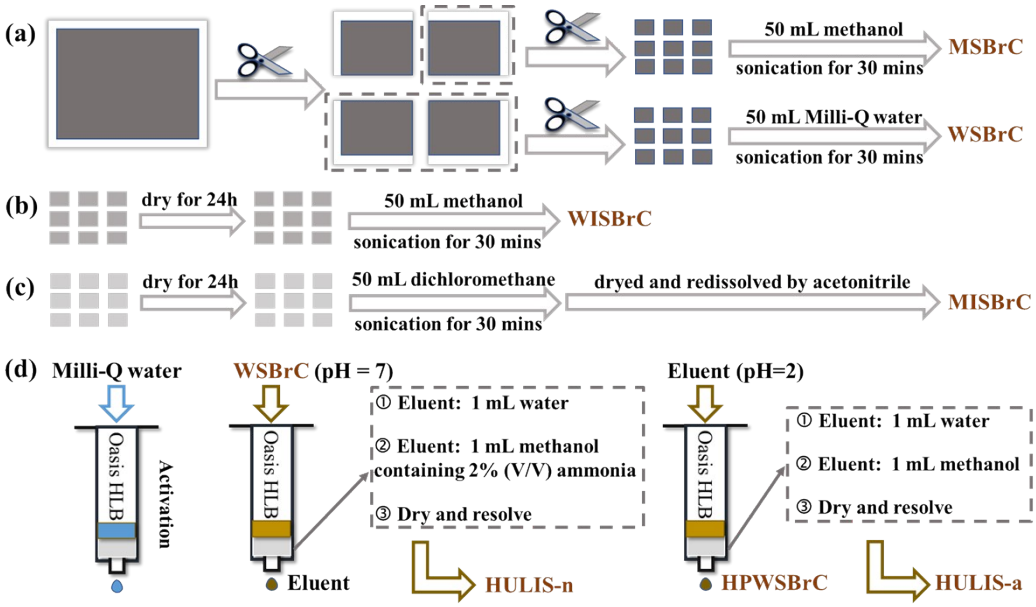

Fig. S2. Separation steps of MSBrC (a), WSBrC (a), WISBrC (b) and MISBrC (c) by sonication extraction, respectively. Separation steps of HULIS (HULIS-n, HULIS-a) and HPWSBrC by SPE method (d).

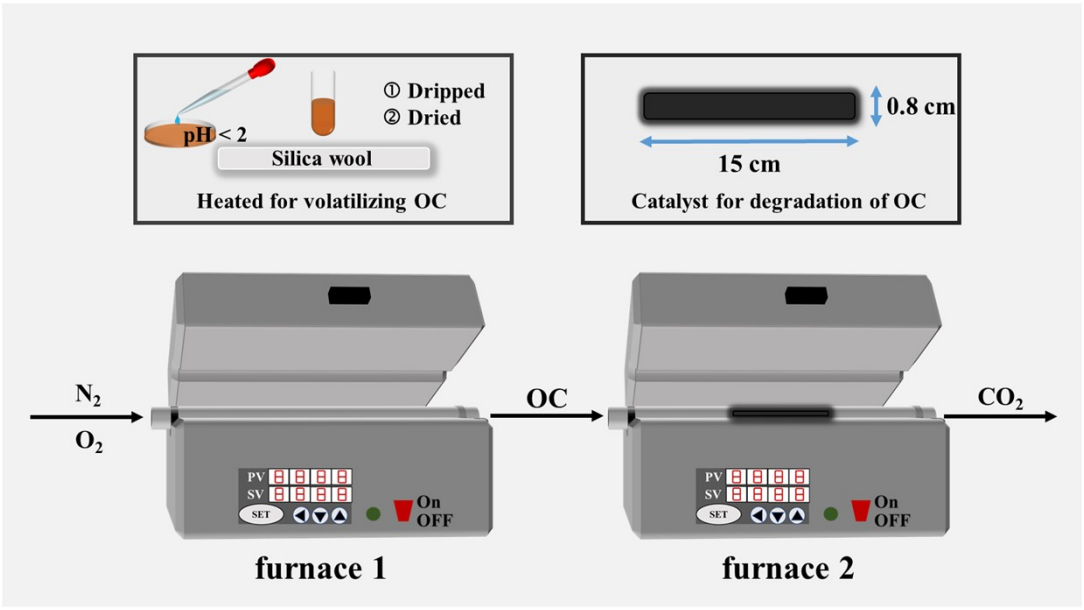

Fig. S3. Schematic diagram of OC concentration detection.

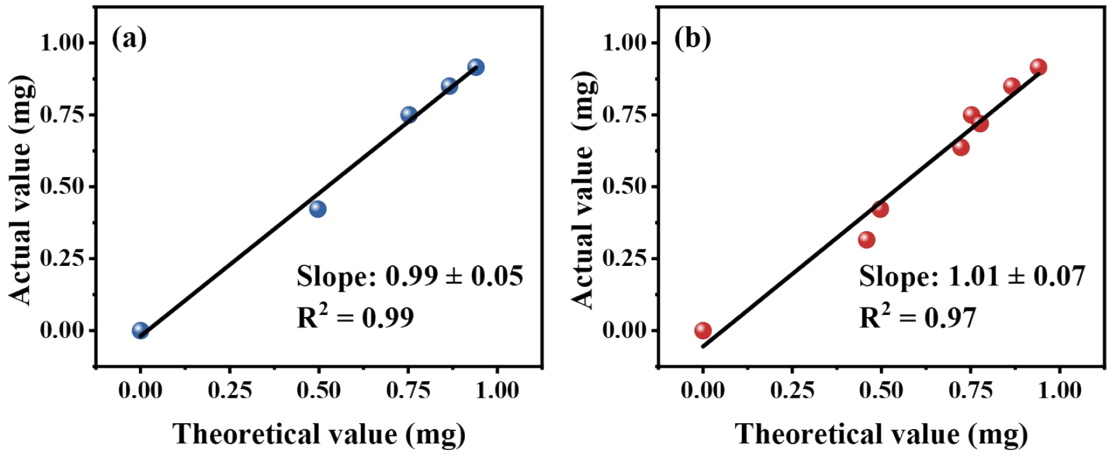

Fig. S4. OC standard curve between actual values measured by GC (mg) and theoretical values (mg) of pyrene (a) and target compounds including pyrene, 9,10-phenanthraquinone, 9-fluorenone, 5-nitroacenaphthene, 9-nitroanthracene, 2-hydroxy-3-nitrobenzoic acid and 2-hydroxy-3-nitrobenzoic acid (b).

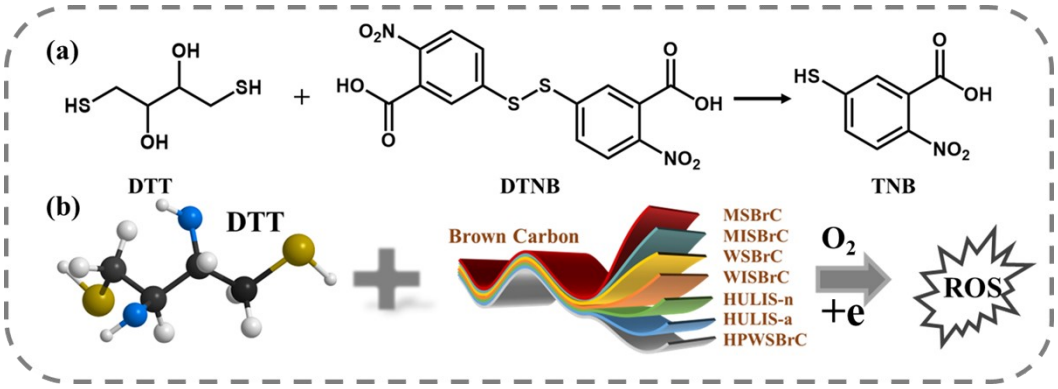

Fig. S5. Reaction mechanism equation of DTT and DTNB for TNB generation (a) and ROS generation mechanism of DTT and BrC extracts (b).

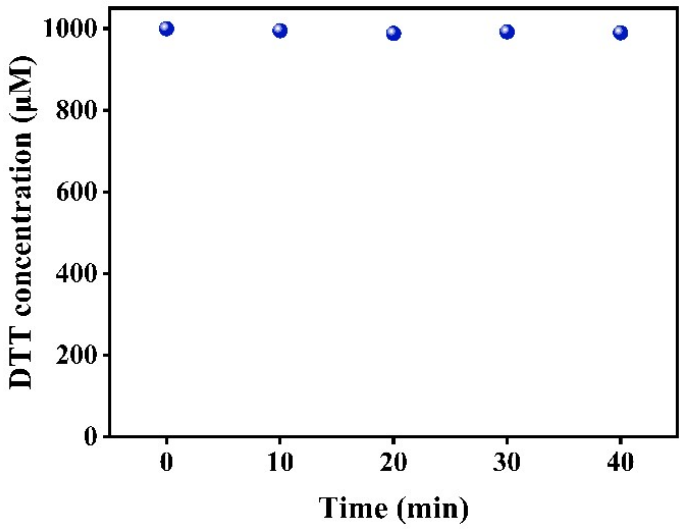

Fig. S6. DTT measurement for 100 μL of methanol mixed with 2.9 mL of Milli-Q water.

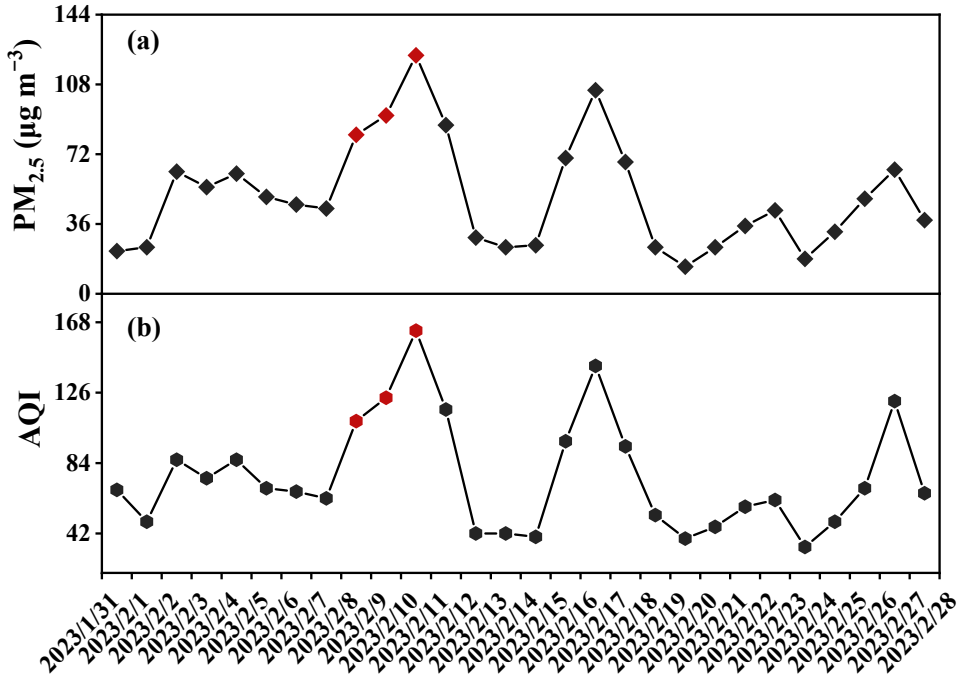

99

100 Fig. S7. $PM_{2.5}$ concentrations and air quality index (AQI) during Feb. 2023.

101

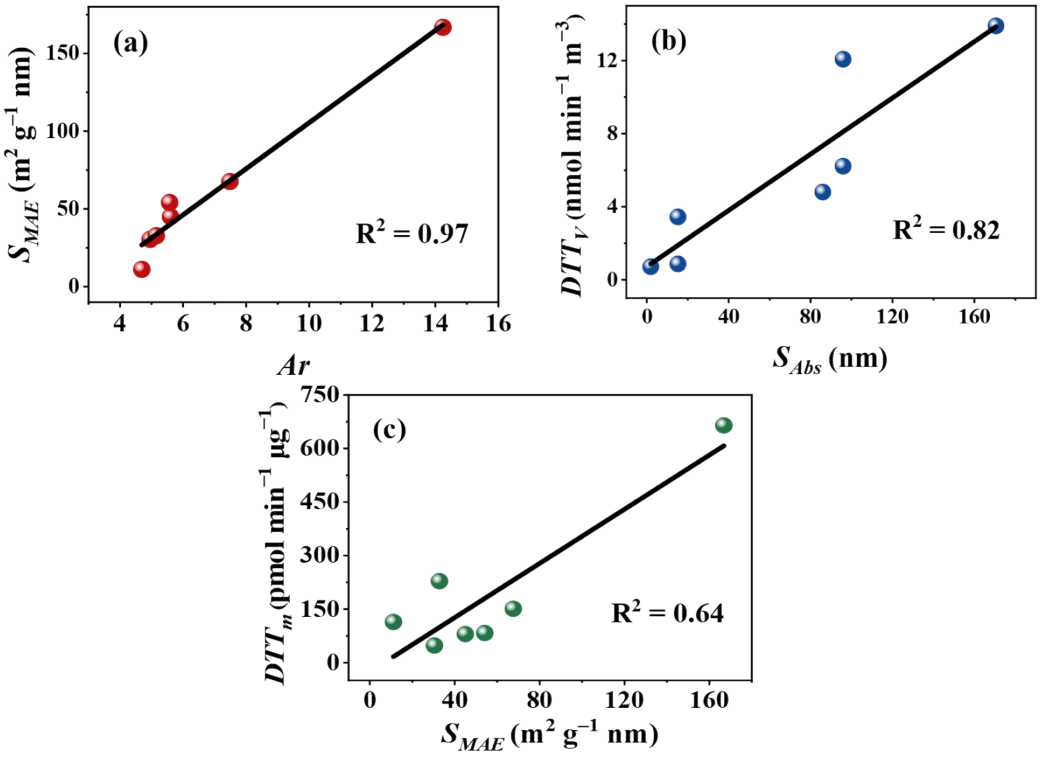

102

103 Fig. S8. Correlation analysis of the integral area of *MAE* (S_{MAE}, m^2 g^{-1} nm) with *Ar* (a).

104 DTT_V (nmol min^{-1} m^{-3}) with the integral area of *Abs* (S_{Abs}, nm) (b). DTT_m with S_{MAE}

105 (c).

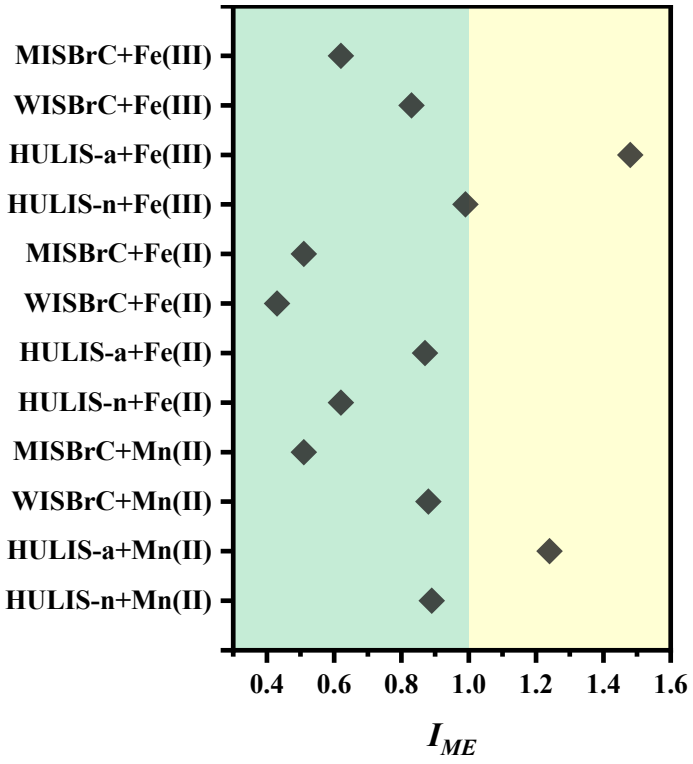

106

107 Fig. S9. The mix effect index (I_{ME}) of metal ions (Fe^{2+}, Fe^{3+} and Mn^{2+}) with the metal

108 free BrC extracts (MISBrC, WISBrC, HULIS-a and HULIS-n).

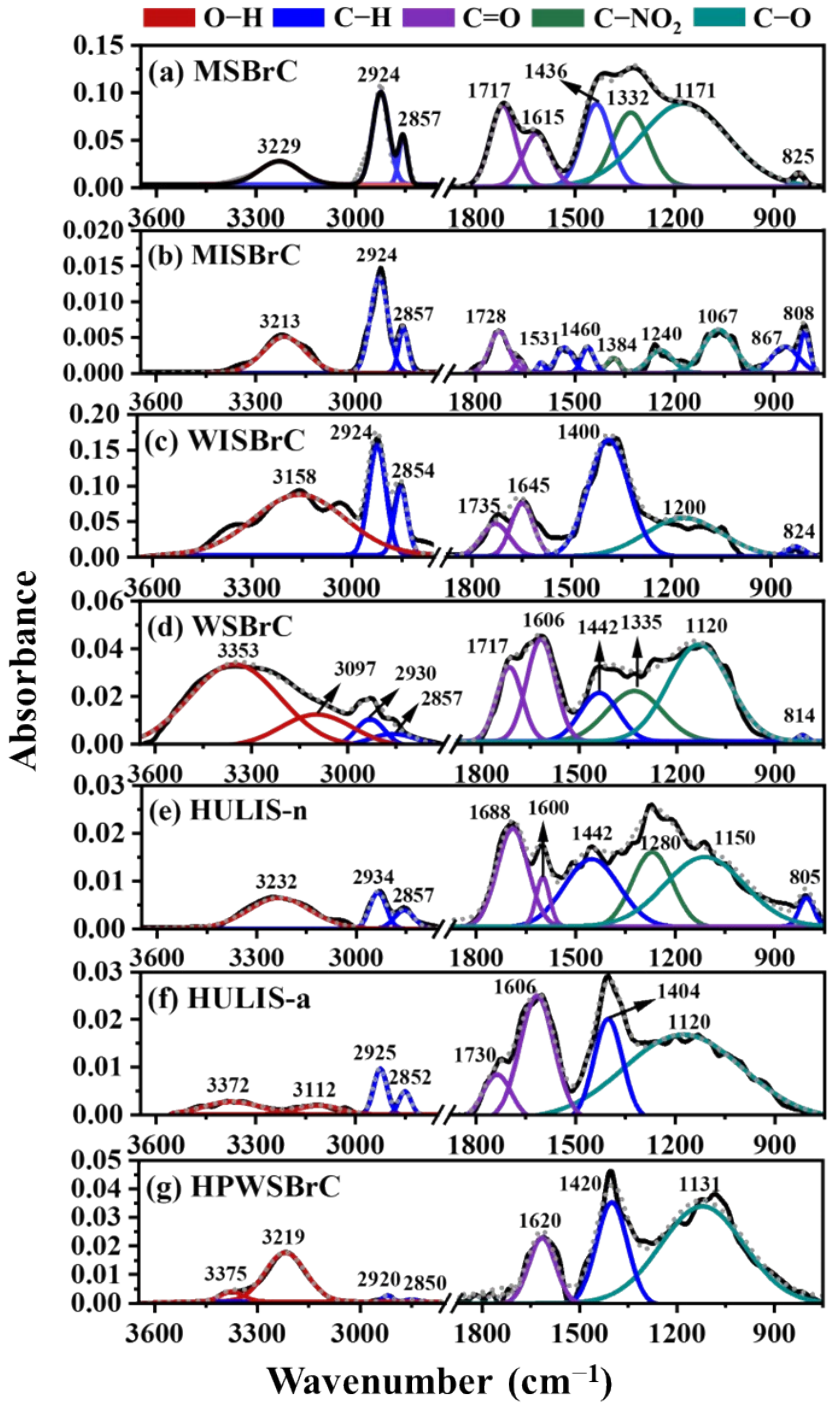

Fig. S10. The curve-fitting of FT-IR spectra of MSBrC (a), MISBrC (b), WISBrC (c), WSBrC (d), HULIS-n (e), HULIS-a (f) and HPWSBrC (g). The black, grey and colorful lines represent the original, fitted and separated spectra, respectively.

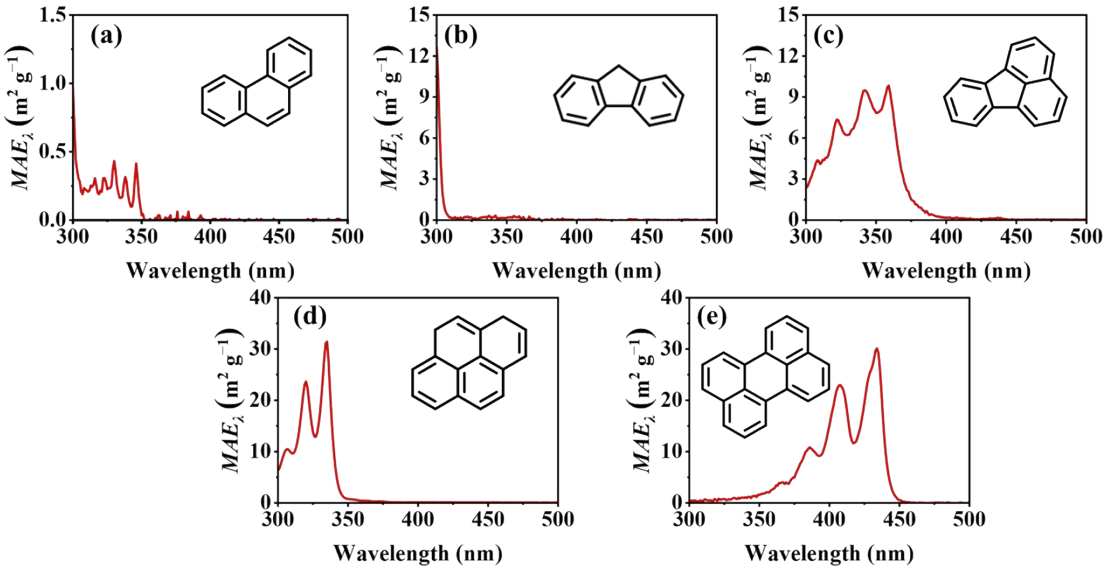

Fig. S11. The *MAE* spectra of phenanthrene (a), fluorene (b), fluoranthene (c), pyrene (d) and perylene (e).

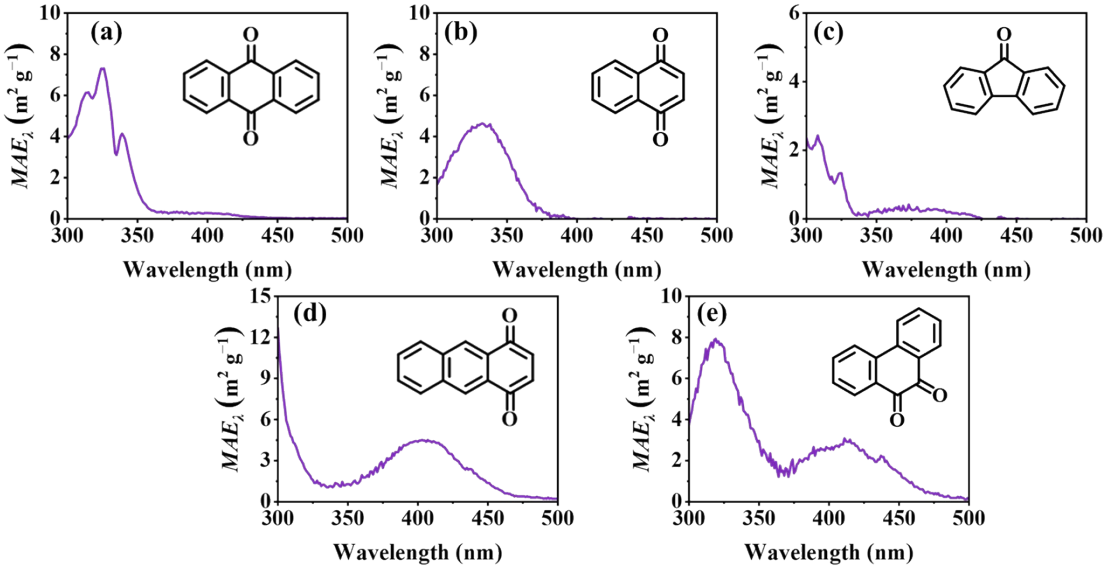

Fig. S12. The *MAE* spectra of anthraquinone (a), naphthalene-1,4-dione (b), 9-fluorenone (c), 1,4-anthraquinone (d) and 9,10-phenanthraquinone (e).

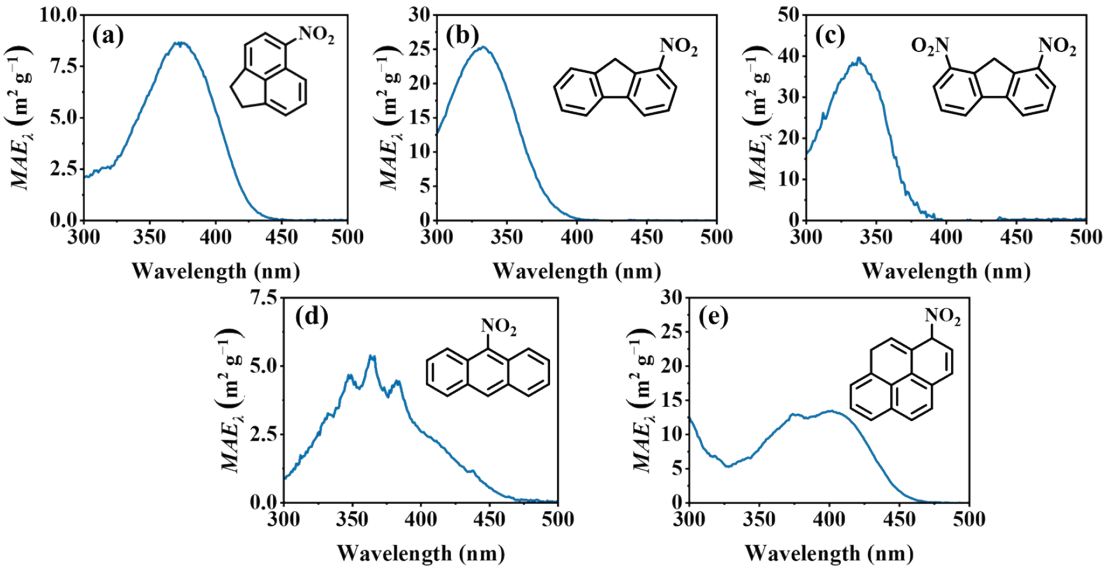

Fig. S13. The *MAE* spectra of 5-nitroacenaphthene (a), 2-nitrofluorene (b), 2,7-dinitrofluorene (c), 9-nitroanthracene (d) and 1-nitropyrene (e).